

Sequential Domain Unfolding in Phosphoglycerate Kinase: Fluorescence Intensity and Anisotropy Stopped-Flow Kinetics of Several Tryptophan Mutants[†]

Joseph M. Beechem,^{*,‡} Mark A. Sherman,[§] and Maria T. Mas^{*,§}

Department of Molecular Physiology and Biophysics, Vanderbilt University, Nashville, Tennessee 37232, and Division of Biology, Physical Biochemistry Section, Beckman Research Institute of the City of Hope, Duarte, California 91010

Received April 14, 1995; Revised Manuscript Received August 29, 1995[⊗]

ABSTRACT: Stopped-flow total intensity and anisotropy experiments on single tryptophan containing mutants of yeast phosphoglycerate kinase (PGK) located in either the carboxy-terminal domain (W308 and W333), amino-terminal domain (W48 and W122), or “hinge” region (W194 and W399) were performed. The results obtained for single tryptophans in individual domains suggest that the unfolding of PGK by guanidinium hydrochloride is a sequential process in which unfolding of the carboxy-terminal domain is followed by the unfolding of the amino-terminal domain. A kinetic intermediate has been detected which consists of an unfolded carboxy-terminal domain and an altered amino-terminal domain, identical in hydrodynamic properties with the native state, but hyperfluorescent. In contrast to the C-terminal tryptophans, which exhibit concurrent total intensity and anisotropy changes in the entire denaturant concentration range (0 → 2 M), the N-terminal tryptophans experience a large increase in fluorescence intensity and a constant anisotropic environment at low concentrations of denaturant, corresponding to the first transition region of the equilibrium unfolding profile. Anisotropy changes for the N-terminal probes are observed above 1 M Gdn-HCl, the region corresponding to the second equilibrium unfolding transition. Stopped-flow experiments performed on PGK mutants with two tryptophans (i.e., with a single tryptophan in each domain) confirm that each domain unfolds independently, and that the individual site-specific mutations do not significantly alter the unfolding pathway. Unfolding kinetics experiments with tryptophans situated in the hinge reveal that the region sensed by W399 unfolds before the carboxy-terminal domain, whereas W194 senses unfolding of both domains.

Phosphoglycerate kinase (PGK)¹ is a well-characterized, two-domain protein. The individual domains are termed the amino-terminal and carboxy-terminal domains, respectively [see Figure 1 in Sherman et al. (1995)]. A “hinge-like” region separates the two domains. In the preceding paper (Sherman et al., 1995) equilibrium unfolding titrations of a variety of single (and double) tryptophan-containing PGK mutants were performed using far-UV CD, near-UV CD, and steady-state plus time-resolved fluorescence. From the equilibrium studies (Sherman et al., 1995), it was proposed that the carboxy-terminal domain is less stable and unfolds before the amino-terminal domain of PGK. The Gdn-HCl-induced transition midpoint for the carboxy-terminal domain is $0.4 \text{ M} < C_m < 0.65 \text{ M}$, whereas the midpoint for the more stable amino-terminal domain is $0.85 \text{ M} < C_m < 1.1 \text{ M}$ [see Table 2 in Sherman et al. (1995)]. To further test this unfolding hypothesis, fluorescence total intensity and anisotropy experiments were performed using stopped-flow techniques. Stopped-flow experiments were performed using Gdn-HCl concentration jumps both above and below the C_m 's

for each domain. “Double-kinetic” experiments were also performed, where picosecond–nanosecond time-resolved data are collected on the millisecond time scale. Single tryptophan mutants located in the amino-terminal domain (W48, W122), the hinge region (W194, W399), and the carboxy-terminal domain were examined (W308, W333) [see Figure 1 in Sherman et al. (1995) for individual tryptophan locations].

Both total intensity and anisotropy data contain information concerning changes in the relative populations of species during a reaction. However, anisotropy data contain additional information describing the average molecular motion which occurs during the lifetime of the excited state. For protein folding reactions, this additional information provides a mechanism in which the average hydrodynamic properties of folding intermediates can be obtained. The rigorous combination of both total intensity and anisotropy stopped-flow data allows one to directly assign quantum yields and anisotropy values to partially folded intermediate states (Otto et al., 1994). The change in stopped-flow anisotropy associated with the individual reporting tryptophans in each domain and hinge region should provide a clear picture concerning the order of domain unfolding in PGK.

EXPERIMENTAL PROCEDURES

Stopped-Flow Fluorescence Detection. Reactions were performed with an SFM-3 stopped-flow unit (Molecular Kinetics, Pullman, WA) with a 50 μL FC.15 fluorescence

[†] J.M.B. was supported by NIH Grants R01 GM45990 and S10 RR05823. M.T.M. was supported by NIH Grant R01 GM41360.

^{*} Corresponding authors. M.T.M.: Telephone, (818) 301-8347; Fax, (818) 301-8891; E-mail, mmas@coh.org. J.M.B.: Telephone, (615) 322-7980; Fax, (615) 322-7236.

[‡] Vanderbilt University.

[§] Beckman Research Institute of the City of Hope.

[⊗] Abstract published in *Advance ACS Abstracts*, October 1, 1995.

¹ Abbreviations: PGK, 3-phosphoglycerate kinase; CD, circular dichroism; Gdn-HCl, guanidine hydrochloride; C_m , guanidine-induced unfolding transition midpoint.

cuvette and hard-stop shutter. Reaction flow rates varied from 2 to 8 mL/s. Reaction time bases depended upon the experiment. Stock solutions of enzyme, dilution buffer, and reaction buffer were loaded into separate syringes. For all experiments, solutions were extensively degassed. All experiments were conducted with a fraction of the data channels devoted to internal controls. For folding and unfolding reactions the internal controls were simply unfolded or folded protein, respectively. These control reactions had absolutely flat anisotropy and total intensity signals. A complete description of the T-format steady-state anisotropy and total intensity fluorimeter can be found in Otto et al. (1994). Briefly, the excitation beam was provided by a 450 W Xenon Arc lamp with a 0.22 m SPEX monochromator (Edison, NJ) whose output was focused onto a fused-silica fiber optic ($10 \times 100 \mu\text{m}$ fiber bundle) and directed into the $50 \mu\text{L}$ stopped-flow observation cuvette after passing through a vertically oriented Oriel film UV linear dichroic polarizer (Stratford, CT, model 27340). On each side of the SFM-3 cuvette head, a home-made emission channel was mounted, consisting of a collimating lens, Glan-Thompson polarizer, and filter holder. The filters utilized were 340 nm cut on type (L34, Hoya optics, Fremont, CA). On the end of each emission channel a R928 photomultiplier tube (PMT) (Hamamatsu Corp.) operating in single-photon counting mode was mounted. The signal from each PMT (measuring light polarized either parallel or perpendicular to the excitation beam) was amplified through an SR455 DC-300 amplifier (Stanford Research, Sunnyvale, CA) and discriminated with an SR400 (Stanford Research) two channel counter. The parallel and perpendicular intensities were simultaneously detected by two MCS-II multichannel scalar cards (Tennelec Nucleus, Oak Ridge, TN) and two 486DX computers. The MCS-II cards were synchronized with the SFM-3 stopped-flow unit through the external sync output from the SFM-3. The excitation polarizer in this stopped-flow instrument is "sandwiched" between the front surface of the observation cuvette and the excitation fiber optic and cannot be easily rotated for horizontal excitation to determine the polarization bias ("G factor") of the instrument. The G factor was therefore obtained by measuring a $3.0 \mu\text{M}$ solution of free tryptophan ($r \approx 0.02$). All reactions were performed at $20 \pm 2^\circ\text{C}$. Multiple kinetic runs (10–15) were summed to obtain adequate signal to noise ratios. Anisotropy and total intensity data were obtained from the parallel and perpendicular channel data using eqs 1 and 2 (see below).

Determination of Kinetic Rates. Empirical exponential fits to single exponentials or sums of exponentials were performed using Sigmaplot 6.0 (Jandel Scientific, San Rafael, CA). Combined global analyses were performed using the Globals Unlimited software package (University of Illinois, Department of Physics, Urbana, IL) modified to include the theory and methods developed in Otto et al. (1994). The fitting parameters for each reaction scheme consist of reaction rates, quantum yields, and steady-state anisotropy values associated with each particular kinetic intermediate.

The steady-state fluorescence total intensity and anisotropy functions were constructed from the individually measured parallel and perpendicular light intensities using eqs 1 and 2, respectively.

$$S = GI_{\parallel} + 2I_{\perp} \quad (1)$$

$$r = (GI_{\parallel} - I_{\perp})/(GI_{\parallel} + 2I_{\perp}) \quad (2)$$

where I_{\parallel} and I_{\perp} are the intensities of fluorescence emitted parallel and perpendicular to the exciting light. G ("G factor") is a term accounting for the bias of the detection system for vertical versus horizontally polarized light.

Determination of the Unfolding Rate of Yeast Phosphoglycerate Kinase (PGK) and Various Tryptophan-Containing Mutants. The rate of unfolding was determined from changes in tryptophan fluorescence. Reactions were performed by mixing (in a 1:1 ratio) $100 \mu\text{L}$ of PGK stock solution with $100 \mu\text{L}$ of Gdn-HCl (0.5–4.0 M). All reactions contained 20 mM sodium phosphate, pH 7.5, and 0.1 mg/mL phosphoglycerate kinase. Gdn-HCl concentrations were determined refractometrically (Pace et al., 1989) using an Abbe Mark II refractometer.

"Double-Kinetic" Experiments. In double-kinetic experiments, picosecond–nanosecond time-resolved fluorescence intensity and anisotropy data are collected on the millisecond time scale (Beechem, 1992; Jones et al., 1995). Briefly, 295 nm 1 ps pulses at 4 MHz (from a Coherent 702 dye laser, synchronously pumped by a Antares Nd:YAG laser) are focused onto the stopped-flow cuvette. Picosecond–nanosecond time-resolved fluorescence data (parallel and perpendicular intensities) are collected in L-format using Glan-Thompson polarizers, a 340 nm filter (L34, Hoya), and a Hamamatsu $6 \mu\text{m}$ microchannel plate detector. Instrument response functions were approximately 60 ps FWHM. Data collection rates were 10–20 kHz. The data were collected into approximately 2000 channels at 12 ps/channel. Typically, the emission polarizer orientation was changed every 25 shots, and a total of 600–1500 shots were collected per experiment in order to achieve sufficient signal-to-noise for the millisecond time slices obtained during the unfolding reactions. Typical peak counts in the total intensity data sets taken every 10–20 ms were 10000 counts.

RESULTS

Stopped-flow fluorescence anisotropy data were obtained on the single tryptophan mutants in the carboxy-terminal domain (W308, W333), the amino-terminal domain (W48, W122), and in the hinge region (W194, W399). The anisotropy changes for the individual site single tryptophans in response to a $0 \rightarrow 1.0 \text{ M}$ Gdn-HCl jump are shown in Figure 1. At this Gdn-HCl concentration, both C-domain tryptophans (W308 and W333) and one hinge tryptophan (W399) indicate that unfolding in the vicinity of the probe has occurred, as evidenced by the change in anisotropy from the native value ($r \approx 0.11$ – 0.16) to that observed in the unfolded state ($r \approx 0.05$). One of the hinge domain tryptophans (W194) indicates partial unfolding. The anisotropy change observed for W399 suggests that complete unfolding in this region occurs within the dead-time of the stopped-flow ($<5 \text{ ms}$). The amino-terminal domain tryptophans (W48 and W122) do not experience any significant change in steady-state anisotropy over this time scale. The steady-state anisotropies of the unfolded mutants are essentially identical ($r \approx 0.05$), whereas the anisotropies for each native mutant are slightly different ($r \approx 0.11$ – 0.16), resulting primarily from differences in mean lifetime and excitation polarization properties.

Although the amino-terminal tryptophans do not undergo any change in anisotropy, they do reveal a relatively large

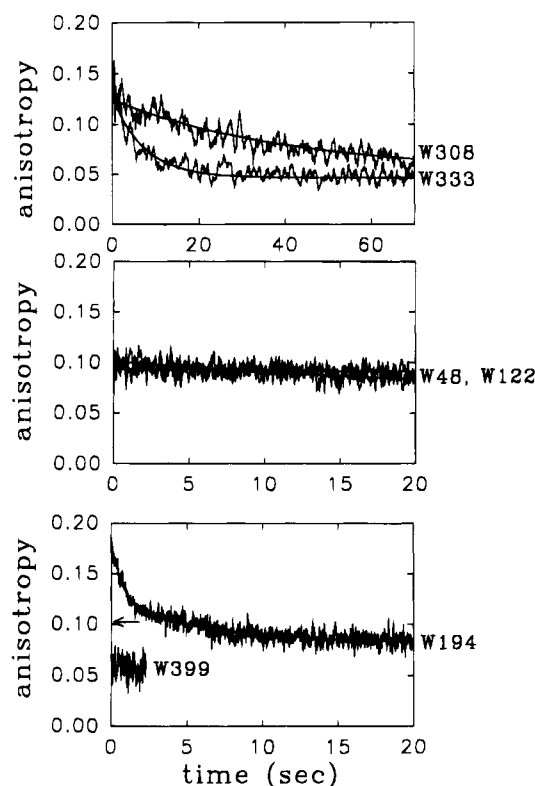


FIGURE 1: Stopped-flow anisotropy kinetics for a $0 \rightarrow 1.0$ M Gdn-HCl jump when examined using site-specific carboxy-terminal domain tryptophans (W308, W333, upper panel), amino-terminal domain tryptophans (W48, W122, middle panel), or hinge region tryptophans (W194, W399, lower panel). The arrow in the lower panel denotes the steady-state anisotropy of W399 in the native form. Excitation wavelength = 295 nm; emission wavelength > 340 nm.

change in total intensity (see Figure 2). The total intensity changes observed for all of the other tryptophan mutants (carboxy-terminal domain and hinge) essentially parallel the anisotropy changes shown in Figure 1. However, the amino-terminal domain tryptophans clearly experience a change in photophysical environment without significant change in rotational environment.

To further examine the overall "stability" of the amino-terminal domain, stopped-flow experiments on W48 and W122 were performed as a function of Gdn-HCl concentration. The results obtained with W48 are shown in Figure 3. At both 0.5 and 1.0 M Gdn-HCl jumps, the observed steady-state anisotropy function is essentially constant. However, as the final Gdn-HCl concentration approaches 1.2 M, the stopped-flow anisotropy pattern begins to change. By 2.0 M Gdn-HCl concentration, the anisotropy signal changes very rapidly. The invariance of the stopped-flow anisotropy of N-domain probes below 1.0 M Gdn-HCl concentration corresponds to the region of the equilibrium unfolding titration tentatively assigned to the carboxy-terminal domain unfolding [$C_m = 0.42$ M (Sherman et al., 1995)]. The anisotropy changes observed for the C-domain tryptophans (Figure 1) are consistent with this assignment. The stopped-flow anisotropy change observed at Gdn-HCl > 1.0 M would correspond to the equilibrium titration phase assigned to the amino-terminal domain unfolding [$C_m = 0.92$ M (Sherman et al., 1995)]. These stopped-flow anisotropy experiments provide strong supporting evidence for the tentative assignments based on the equilibrium unfolding results.

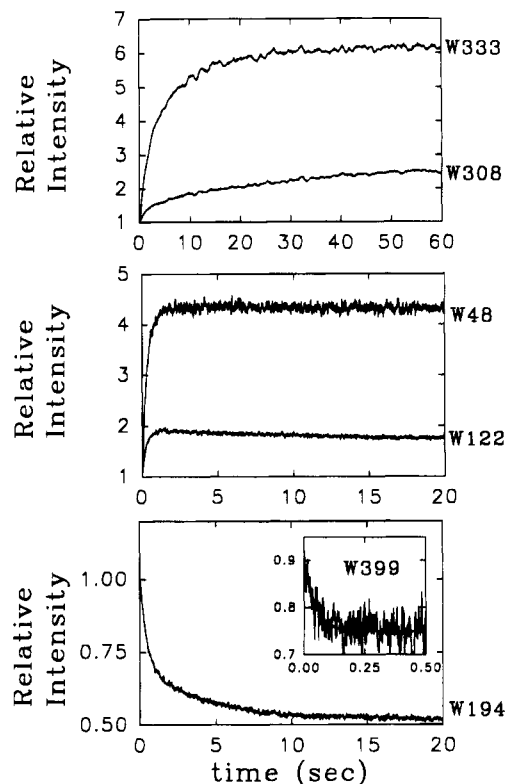


FIGURE 2: Stopped-flow total intensity kinetics for a $0 \rightarrow 1.0$ M Gdn-HCl jump when examined using site-specific carboxy-terminal domain tryptophans (W308, W333, upper panel), amino-terminal domain tryptophans (W48, W122, middle panel), or hinge region tryptophans (W194, W399, lower panel). The inset in lower panel shows the very fast quenching observed for W399 upon unfolding. Excitation wavelength = 295 nm; emission wavelength > 340 nm.

The total intensity stopped-flow pattern for W48 (Figure 3, bottom) depends on the denaturant concentration. At lower Gdn-HCl concentrations jumps (0.5 and 1.0 M) the total intensity signal increases 40% and 100%, respectively. As the final Gdn-HCl concentration is further increased, this rapid increase in total intensity becomes too fast to resolve in the stopped-flow, and by 2.0 M one can only observe the slower decreasing phase in total intensity. Combined simultaneous analysis of this total intensity and anisotropy data (Otto et al., 1994) reveals that all total intensity transitions require at least two kinetic phases (fast and slow). Both kinetic phases are Gdn-HCl concentration dependent (see Figure 4). Under 1.2 M Gdn-HCl, the anisotropy associated with each kinetic phase is identical, revealing that the rotational environment of the N-domain probes remains unchanged. The unfolding kinetics at 1.2 M Gdn-HCl reveal that the rapid increase in relative quantum yield ($k = 13$ s⁻¹) is not associated with a large change in anisotropy. This species has a quantum yield of 1.9 times that of the native enzyme, but with the same anisotropy value. We term this species, which represents an altered state of the amino-terminal domain that exists when the carboxy-terminal domain has apparently unfolded [Figure 2 and Sherman et al. (1995)], a hyperfluorescent intermediate. It is clear that the rotational environment sensed by the tryptophan (W48) in this altered amino-terminal domain is very similar to that experienced in the native state (further experiments addressing this point will be described below). The slower kinetic phase ($k = 0.2$ s⁻¹) has a decreased relative quantum yield (from 1.9 to 1.4 times native) and an anisotropy value ($r =$

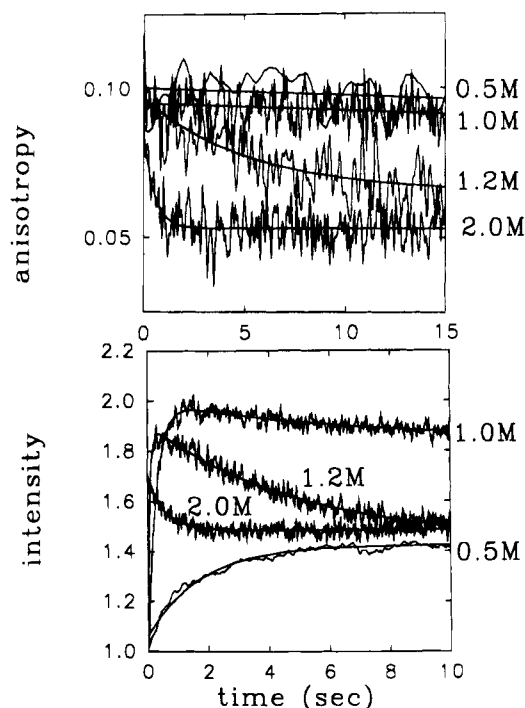


FIGURE 3: Stopped-flow total intensity (lower) and anisotropy (upper) kinetics as a function of different Gdn-HCl concentration jumps for the amino-terminal domain tryptophan W48. Smooth lines through the data represent simultaneous fitting of both total intensity and anisotropy data using the method of Otto et al. (1994). The recovered rate constants can be found in Figure 4. Excitation wavelength = 295 nm; emission wavelength > 340 nm. For visualization, the time scale for the 0 \rightarrow 2.0 M jump is expanded by 4 \times (15 s on the graph is actually 3.75 s).

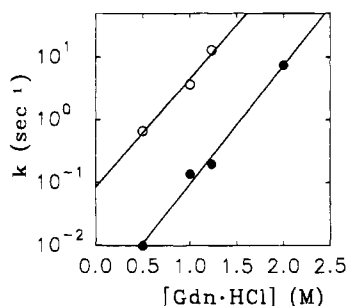


FIGURE 4: Recovered rate constants for the unfolding of W48 as a function of Gdn-HCl concentration. (O) Formation of hyperfluorescent intermediate; (●) final unfolding phase of amino-terminal domain.

0.05) characteristic of the unfolded species. For this system, the phase associated with a decrease in fluorescence intensity is directly associated with a decrease in steady-state anisotropy. The steady-state anisotropy of the hyperfluorescent state is identical to that of the native enzyme. By 2 M Gdn-HCl, the formation of the hyperfluorescent state occurs within the dead-time of the stopped-flow instrument (<5 ms). The only phase which can now be resolved is the unfolding of the hyperfluorescent intermediate. The logarithm of both the fast and slow unfolding rates are linear in Gdn-HCl, with a slope of approximately 2.0 (Figure 4). A question arises concerning how such a large change in total intensity can occur with essentially no change in steady-state anisotropy.

To examine this effect in more detail, "double-kinetic" experiments were performed, where the fluorescence lifetime-(s) are directly measured as a function of the millisecond

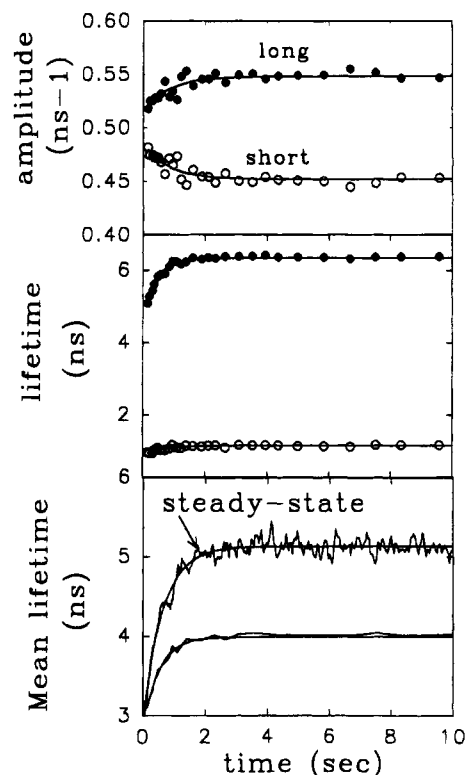


FIGURE 5: Recovered nanosecond time-resolved amplitude (upper) and fluorescence lifetime terms (middle) as a function of millisecond unfolding of W48 PGK in response to a 0 \rightarrow 1.0 M Gdn-HCl jump. Lower panel shows the steady-state fluorescence change (approximately 70% increase) and the mean lifetime change calculated as $\langle\tau\rangle = (\sum \alpha_i \tau_i) / (\sum \alpha_i)$. To allow for a direct comparison, the steady-state intensity (arbitrary units) is normalized to the same value (3) as the mean lifetime (approximately 3 ns) at time zero.

unfolding time-scale (Beechem, 1992; Jones et al., 1995). These results are shown in Figure 5. One can see that although there is a relatively large change in total intensity (Figure 5, lower panel), the mean lifetime only changes 25%, and no change in the time-resolved anisotropy function was observed (data not shown). This small change in mean lifetime ($\langle\tau\rangle$) with no concomitant change in mean rotational correlation time ($\langle\phi\rangle$) will decrease the steady-state anisotropy (r_{ss}) value by only 0.004 units (using Perrin's equation): $r_{ss} = r_0 / (1 + \langle\tau\rangle / \langle\phi\rangle)$. This small change is well within the errors associated with the essentially constant anisotropy which is observed for this Gdn-HCl concentration jump (0 \rightarrow 1 M). At this concentration of Gdn-HCl, the double-kinetic lifetimes observed during the first 10 s of unfolding represent the lifetimes associated with the hyperfluorescent intermediate. The very slow transition from the hyperfluorescent state to the more quenched unfolded state requires several minutes. The rate constants observed for the formation of the hyperfluorescent intermediate are essentially identical for all of the double-kinetic markers (amplitudes, lifetimes, or mean lifetime), revealing that the formation of this state may be a single-step kinetic process. From these data, the observed increase in fluorescence intensity can be partitioned into approximately 40% changes in dynamic quenching and 60% static quenching terms (Figure 5, bottom panel). Similar experiments performed on W122 reveal an almost identical pattern (data not shown).

The double tryptophan containing mutants show intermediate stabilities between the single mutants (Sherman et al.,

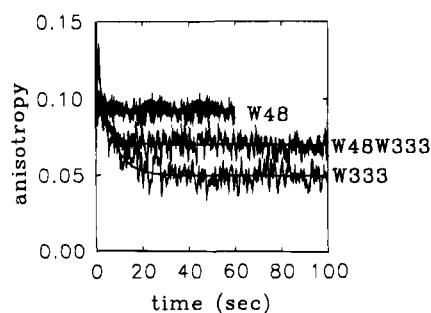


FIGURE 6: Stopped-flow fluorescence anisotropy kinetics observed using the amino-terminal domain (W48), carboxy-terminal domain (W333), and the two-tryptophan containing mutant (W48/W333). $0 \rightarrow 1.0$ M Gdn-HCl concentration jump; 295 nm excitation; >340 nm emission.

1995). If each tryptophan were acting independently (i.e., exhibiting the same behavior as in the corresponding single tryptophan mutants), the stopped-flow unfolding anisotropy traces of these double-tryptophan mutants should reveal behavior which has identical kinetics to the linear superposition of the individual site mutants. These data are shown in Figure 6. As expected, the kinetics of the W48/W333 double tryptophan containing mutant has anisotropy unfolding kinetics with two phases: a fast phase reported by W333 and an invariant anisotropy associated with the amino-terminal probe (W48), followed by a slow phase. The kinetics of the fast anisotropy phase in the double-tryptophan W48/W333 mutant are identical to that obtained with the W333 single-tryptophan mutant. These data are completely consistent with the ordered unfolding of the carboxy-terminal domain prior to unfolding of the amino-terminal domain.

DISCUSSION

Wild-type PGK has two intrinsic tryptophans, both located with the carboxy-terminal domain [W333 and W308; see Figure 1 in Sherman et al. (1995)]. Extensive unfolding studies with the wild-type enzyme found that the CD and fluorescence transitions were essentially coincident and obeyed classic two-state behavior (Szpirowska et al., 1994), with very high cooperativity (i.e., the slope of the two-state transition is very steep). Single-tryptophan mutants (W308 and W333) and a no-tryptophan mutant (W-) of yeast PGK were also examined and found to obey two-state behavior, with slightly altered stability compared to the wild-type (Szpirowska et al., 1994). Interpretation of this early work involved a model where both domains were acting together in a highly cooperative manner. Careful re-examination of the CD-monitored unfolding data for the W-, W308, and W333 mutants reveals that there is a trace of a very small amplitude transition at about 1 M (Sherman et al., 1995). This effect can essentially be eliminated by baseline subtraction with linear extrapolation of the signal as a function of denaturant concentration. In fact, it is often difficult to know when the linear extrapolation and baseline correction term is working correctly or actually acting to hide a real transition. A hyperfluorescent intermediate was detected under equilibrium unfolding conditions using additional single tryptophan probes (Sherman et al., 1995). The results of these equilibrium unfolding studies suggest a sequential unfolding model, with the C-terminal domain unfolding prior to the N-terminal domain.

In this work, several single tryptophan mutants were examined in which tryptophan probes had been strategically located in widely separated positions within the amino-terminal domain (W48, W122) and the hinge region (W194, W399) as well as in the carboxy-terminal domain (W308, W333). In order to test for the presence of kinetic unfolding intermediates, stopped-flow fluorescence total intensity and anisotropy kinetic experiments were performed on each of these mutants. Finally, in order to understand the photophysical details associated with the changes in fluorescence lifetime parameters during unfolding, "double-kinetic" experiments were performed for the N-domain spectroscopic probes.

The experimental result which proved crucial for constructing an initial hypothesis of a sequential domain unfolding mechanism for PGK is shown in Figure 1. The stopped-flow anisotropy unfolding data using a $0 \rightarrow 1$ M Gdn-HCl jump falls into three very distinct classes. The anisotropy change found in the carboxy-terminal domain mutants (W308 and W333) reflects a relatively rapid and complete unfolding transition, with W333 having faster unfolding kinetics than W308 within the same domain. The anisotropy change observed in the amino-terminal domain mutants (W48 and W122) reveals essentially no change in anisotropy function over the same time scale. The hinge mutants reveal intermediate changes. The hinge region sensed by W399 appears to be completely unfolded within the dead-time of the stopped-flow, whereas unfolding of the hinge region reported by W194 is intermediate, with a partial unfolding transition occurring on a time-scale similar to W333, but with a high limiting anisotropy similar to the amino-terminal domain anisotropy signal.

The importance of obtaining stopped-flow anisotropy data on this system is clearly illustrated by examining the total intensity versions of the same experiment (Figure 2). Rather remarkably, the total intensity data from the amino-terminal domain tryptophans reveal the fastest signal change. Although in many protein systems which have been examined in the past, the change in total intensity was simply equated with the fraction unfolded, such an assignment would be absolutely incorrect in this case.

In order to obtain a better understanding of the $0 \rightarrow 1.0$ M Gdn-HCl stopped-flow anisotropy results (i.e., invariant anisotropy of the N-domain spectral probes), a series of Gdn-HCl concentration jumps were examined. These results for the W48 mutant are shown in Figure 3. It was found that the stopped-flow anisotropy kinetics are invariant at Gdn-HCl jumps in the concentration range of the first equilibrium unfolding transition characterized in the preceding paper [Figure 2 in Sherman et al. (1995)]. However, as the Gdn-HCl concentrations are varied in the region associated with the second (higher C_m) transition, anisotropy changes are observed, indicating unfolding of N-terminal domain. The concentration dependence of the total intensity stopped-flow experiments can also be interpreted within this model (Figure 3, lower). At lower Gdn-HCl jumps, one can clearly resolve the formation of the hyperfluorescent intermediate. There is no anisotropy change occurring at these low Gdn-HCl concentrations. The carboxy-terminal domain is unfolding in this concentration range (Figures 1 and 2). The kinetics of the formation of this hyperfluorescent intermediate, however, is faster than the unfolding of the carboxy-terminal domain (compare Figure 2 middle with upper). Therefore,

the unfolding of the carboxy-terminal domain itself does not produce the hyperfluorescent state. As the Gdn-HCl concentration increases, the formation of the hyperfluorescent state is pushed into the dead-time of the stopped-flow (<5 ms). At these higher Gdn-HCl concentrations, the stopped-flow anisotropy decrease is clearly linked to the decreasing phase in the total intensity function.

The "double-kinetics" result shown in Figure 5 explains how this large change in total intensity can be associated with no change in steady-state anisotropy. The change in total intensity was resolved into static and dynamic components. Only 40% of the observed steady-state total intensity change is dynamic in nature, i.e., mean lifetime follows the dynamic contribution of the total intensity change. The additional 60% change in the steady-state intensity (which is not observed in the time-resolved signal) arises from changes in static quenching components which do not alter the mean lifetime. The mean lifetimes of the various single tryptophan mutants are all relatively short with respect to the global tumbling of PGK. In W48, the mean-lifetime changes from approximately 3 to 4 ns (30% change) within the first 1 s of unfolding (Figure 5, lower panel). The steady-state total intensity function changes are more than twice as large (70%). With these photophysical characteristics, W48 represents a very nice spectroscopic marker whose signal changes are almost completely (?) dominated by localized changes in the amino-terminal domain. Therefore, it was very reassuring to find that W122, located at the exact opposite side of the amino-terminal domain [Figure 1 in Sherman et al. (1995)] revealed an almost identical pattern (data not shown). Both reveal two total intensity transitions, with an increasing and a decreasing phase. Both have invariant anisotropies when examined through the increasing total intensity change region, and both reveal unfolding in the higher Gdn-HCl concentration range. Therefore, formation of the hyperfluorescent intermediate state must involve a change in the photophysical environment associated with "both ends" of the amino-terminal domain. It seems likely that this transition is occurring over the entire amino-terminal domain.

The combined use and simultaneous analysis of fluorescence stopped-flow total intensity and anisotropy data has just recently been described (Otto et al., 1994). With this analysis it is possible to unravel complex patterns of changes in anisotropy and total intensity functions in terms of internally consistent sets of kinetic and spectroscopic parameters. The combined data for PGK, however, are so clear that this analysis methodology, although it was utilized, was not absolutely necessary. Since the photophysical intensity

change associated with the amino-terminal domain tryptophans was found to be totally decoupled from the anisotropy change, the simplest explanation of these data is that the amino-terminal domain does not globally unfold during this first transition. Rigorous data analysis yields very good fits to this type of model (smooth lines in Figure 3). The high-resolution time-resolved equilibrium titration data are entirely consistent with this interpretation [see Figure 3 in Sherman et al. (1995)]. The double-kinetic data reveal that decoupled signals of this type would be predicted from the relatively small changes in the observed mean fluorescence lifetime. The data from the two-tryptophan containing mutants support the interpretation that the spectroscopic probes themselves are not causing this anomalous behavior.

No attempt has been made to interpret the differences in absolute rates observed between spectroscopic markers located within the same domain. For instance, it is clear that the carboxy-terminal domain tryptophan W333 reports faster unfolding at any given Gdn-HCl concentration than the carboxy-terminal domain tryptophan W308 (see upper panel of Figure 1). Similarly, W122 in the amino-terminal domain consistently reports faster unfolding than W48 (data not shown). A simplistic interpretation of these data would be that unfolding of the extended loop region of the amino-terminal domain (near W122) occurs earlier than unfolding of the region sensed by W48. Similarly, changes reported by the tryptophans situated in the C-terminal domain might suggest that unfolding of the region around W333, which is closer to the hinge, occurs earlier than unfolding of the region around W308. Answering which domain unfolds first can be performed in a relatively straightforward manner, but identifying the subregions within each domain that fold/unfold first will require additional site-specific mutants, as will a detailed characterization of unfolding events within the hinge region.

REFERENCES

- Beechem, J. M. (1992) *Proc. SPIE* 1640, 676–681.
- Jones, B. E., Beechem, J. M., & Matthews, C. R. (1995) *Biochemistry* 34, 1867–1877.
- Otto, M. R., Lillo, M. P., & Beechem, J. M. (1994) *Biophys. J.* 67, 2511–2521.
- Pace, C. N., Shirley, B. A., & Thomson, J. A. (1989) in *Protein Structure: A Practical Approach* (Creighton, T. E., Ed.) pp 311–330, IRL Press, Oxford, U.K.
- Sherman, M. A., Beechem, J. M., & Mas, M. T. (1995) *Biochemistry* 34, 13934–13942.
- Szpikowska, B. K., Beechem, J. M., Sherman, M. A., & Mas, M. T. (1994) *Biochemistry* 33, 2217–2225.

BI950842O